Identification and preparation of stable water dispersions of protein - Carbon nanotube hybrids and efficient design of new functional materials

# Identification and Preparation of Stable Water Dispersions of Protein - Carbon Nanotube Hybrids and Efficient Design of new Functional Materials

*Matteo Di Giosia,[†] Francesco Valle,[‡] Andrea Cantelli, [†] Andrea Bottoni,[†] Francesco Zerbetto,[†] Elisa Fasoli,[§] Matteo Calvaresi, [†,*]*

[†] Dipartimento di Chimica "G. Ciamician", Alma Mater Studiorum - Università di Bologna, V. F. Selmi 2, 40126 Bologna, Italy

[‡]Istituto per lo Studio dei Materiali Nanostrutturati (CNR-ISMN), Consiglio Nazionale delle Ricerche, via P. Gobetti 101, 40129 Bologna, Italy

[§] Dipartimento di Chimica, Materiale e Ingegneria Chimica "Giulio Natta", Politecnico di Milano, 20131 Milano, Italy

*Corresponding author: Phone: +390512099478 E-mail: matteo.calvaresi3@unibo.it (Matteo Calvaresi)

ABSTRACT

Carbon nanotubes, CNTs, and proteins could not be more chemically and physically distant. CNTs are hardly soluble and strongly hydrophobic. They are smooth wires, mechanically strong, with electronic properties that make them unique. Many proteins are water soluble and hydrophilic. They are highly corrugated and elastic. They can recognize a target molecule with high selectivity and sensitivity and can have catalytic activity. Integration of the remarkably different features of CNTs and proteins would create a new class of multifunctional materials. The *conundrum* to solve lies in how to best match proteins and CNTs. High-throughput virtual screening is used to predict the ability of 1207 proteins to recognize carbon tubes with a well-defined 1.3 nm diameter.

The propensity for formation of protein-CNT hybrids is ranked. Experiments carried out in this work validated the computational results and show that the identified proteins are able to bind and disperse in water the selected CNTs. The highest scoring proteins are further examined in detail to identify general rules for binding and discussed for a variety of practical applications.

## 1. INTRODUCTION

The properties of carbon nanotubes and proteins differ greatly. Chemically, CNTs are deceivingly simple objects made only by carbon atoms arranged in a cylindrical structure. They can be considered hydrophobic wires with noteworthy mechanical and electrical properties. Proteins are "soft materials" with a stunning assortment of chemical and physical features that offer a variety of shapes and sizes. In their "living watery environment", proteins recognize selectively, among zillions of molecules, their own substrate and perform chemical reactions with very high efficiency. Even if proteins and CNTs are so different, the similarity of their size, or "commensurability", makes possible for CNTs and proteins to interact and form hybrid systems. The assembly of these hybrids is governed by the surface chemistry of both parties, and a variety of different chemical interactions (π–π stacking, hydrophobic, surfactant-like and charge-π interactions) make possible their formation and technological exploitation [1–7].

The existence of these types of interaction does not guarantee *per se* binding of a protein to a CNTs. Proteins with similar percentages of a given residue bind differently to CNTs [8] because of the spatial organization. Recently, we highlighted the role of shape complementarity as the crucial factor controlling the binding between proteins and nanoobjects [9,10].

During the last few years, two approaches have emerged to create functional nano-bio interfaces: *de novo* design [11,12] and systematic screening [13–17], both at the experimental [13,14] and computational [15–17] level. The intent of this work is to lay the ground for a systematic computational approach able to screen a database of proteins to identify CNT binding proteins. Techniques to identify potential binders are used in the drug discovery process, where a large database of ligands is screened to identify the best candidate to bind to a specific target [18]. The process can be inverted and a protein database can be screened to select proteins able to recognize an individual molecule [19,20]. Docking protocols build the geometries of interaction (or poses) and quantify the interactions, giving as a result a rank of the possible binders [19,20]. The predictive ability of docking algorithms was already demonstrated for protein-carbon nanoparticles interactions. [9,10, 15-17, 21-40]

In the present paper, to investigate the nature and importance of the interactions between proteins and CNTs, representative CNTs of ca. 1.3 nm of diameter, and a protein database, namely PDTD [41], were chosen. The choice of 1.3 nm diameter is due to the fact that these tubes are commercially available with a well-defined diameter range.

The well-defined diameter range of the selected CNTs used in the virtual screening process will also offer the possibility to test the predictive power of the protocol, in fact some of the identified proteins were tested to check their ability to bind CNTs. All the tested proteins bind to the selected CNTs, as showed by AFM measurements.

The development of these hybrid CNT-protein systems may potentially combine CNTs and proteins properties and drive fundamental technological advancements in different fields of nanotechnology, medicine, materials science, and biology [1–7]. For the identified complexes a MM-GBSA analysis [42,43] of the structures in their minimized

geometries provides a quantitative description of the CNT-binding pocket and identifies the most effectively interacting residues [9,10,25,44,45].

## 2. MATERIALS AND METHODS

### 2.1 COMPUTATIONAL DETAILS.

**Generation of the poses.** Docking models were obtained using the PatchDock algorithm [46]. PatchDock takes as input two molecules and computes three-dimensional transformations of one of the molecules with respect to the other with the aim of maximizing surface shape complementarity, while minimizing the number of steric clashes. Given a protein and a molecule, PatchDock first divides their surfaces into patches according to the surface shape (concave, convex, or flat). Then, it applies the geometric hashing algorithm to match concave patches with convex patches and flat patches with flat patches and generates a set of candidate transformations. Each candidate transformation is further evaluated by a set of scoring functions that estimate both the shape complementarity and the atomic desolvation energy [47] of the complex. These terms are the most important in the case of binding of carbon nanotubes with proteins. Redundant solutions are discarded by use of rmsd (root-mean-square deviation) clustering. PatchDock is highly efficient, because it utilizes advanced data structures and spatial pattern detection techniques, which are based on matching of local patches. The local shape information is then extended and integrated to achieve global solutions. The algorithm implicitly addresses surface flexibility by allowing minor penetrations.

**Scoring of the poses.** Accurate rescoring of the complexes is then carried out using FireDock program [48]. This method simultaneously targets the problem of flexibility and scoring of solutions produced by fast rigid-body docking algorithms. Possible

readjustments of the protein structure in the presence of the solvent are accounted for. Redundant entries are present in the database for proteins known to be flexible, sidechain flexibility is modeled by rotamers and Monte Carlo minimization [49].

Following the rearrangement of the side-chains, the relative position of the docking partners is refined by Monte Carlo minimization of the binding score function.

Of course, the replacement of computationally more expensive dynamics methods by Monte Carlo minimization is only a partial solution for protein unwrapping on CNT surface [50].

Desolvation free energy in the binding process is taken into account by a solvation model using estimated effective atomic contact energies (ACE) [47]. All the candidates are ranked by a binding score [48]. This score includes, in addition to atomic contact energy used to estimate the desolvation energies [47], van der Waals interactions, partial electrostatics, explicit hydrogen and disulfide bonds contribution. In addition three additional components to the total binding score are added: $E_{\pi-\pi}$ for the calculation of the $\pi-\pi$ interactions, $E_{cation-\pi}$ for the calculation of the cation$-\pi$ interactions and $E_{aliph}$ for the calculation of hydrophobic interactions. These energetic components are crucial to describe:

i) the interactions that occur between the aromatic residues Trp, Phe, Tyr, His, and the CNT wall surface

ii) the interactions of the positive amines of Lys or Arg with the $\pi$-electron cloud of the CNTs (Phe, Tyr, Trp),

iii) the hydrophobic interactions that involve aliphatic residues as Met, Leu, Ile, Pro, Val, Ala.

**Minimizing the pose.** The best poses for every selected protein were full minimized by AMBER 12 [51]. The ff12SB force field [51] was used to model the proteins, while

the CNT atoms were modeled as uncharged Lennard–Jones particles by using the CA atom type (sp2 aromatic carbon parameter), from the AMBER force field. Picking available parameters from existing [9,52,53] or AMBER[15,54,55] force fields is a common strategy applied to describe carbon nanoparticles. Polarizable force fields may improve the description of the interactions betweens CNTs and biomolecules [56], but they are not applicable for massive database analysis.

The minimization was carried out with sander, using the GB (Generalized Born) model [57,58] for the solvation and no cut-off for van der waals and electrostatic was used.

**MM-GBSA analysis.** In order to identify the residues responsible for the binding of the proteins to the CNT, we carried out a decomposition analysis of the minimized structure according to the MM-GBSA scheme [42,43]. The per-residue decomposition analysis provides the contribution of the individual amino acids in the binding.

2.2 EXPERIMENTAL DETAILS.

**Materials.** Commercially available CNTs of 1.3 nm, produced by the CoMoCAT catalytic CVD process (80% purity), were obtained from Sigma (code 724777). All the proteins were obtained from Sigma as lyophilized powders, and used as supplied: glutathione S-transferase from equine liver (G6511), lysozyme from chicken egg white (L6876), carbonic anhydrase from bovine erythrocytes (C2624), hexokinase from *Saccharomyces cerevisiae* Type III (H5000), bovine serum albumin (A2153), α-amylase from hog pancreas (10080).

**Proteins-CNT Preparation.** Proteins-CNT hybrids were prepared by addition of 1.5 mg of CNT powder, used as commercially available, without any additional purification, in a 3 mg/ml solution (1ml) of protein in Milli-Q water. After sonication for 60 min using a probe tip sonicator (Hielscher Ultrasonic Processor UP200St, equipped with a sonotrode S26d7, used at 40% of the maximum amplitude) in an ice

bath, CNTs were dispersed in the protein solution forming a black mixture. A black solution was obtained after centrifugation at 10000g for 10 min and collection of the supernatant. UV-vis absorption spectra were recorded at 25 C by means of Agilent Cary 60 UV-Vis Spectrophotometer.

**AFM experiments.** AFM (Digital Instruments, Multimode VIII equipped with a Nanoscope V) operated in ScanAsyst mode was used to analyze the dispersion state of the tubes. The samples for AFM measurements were prepared by drop casting 5 µl of proteins-CNT hybrids solution onto a freshly cleaved mica substrate for 10 min then rinsed with milliQ water and dried with a stream of $N_2$. The experiments in liquid were carried on in a similar way, but the sample was never dried and it was plugged in the AFM fluid cell where the appropriate buffer solution was then injected. The liquid in the fluid cell was changed using a syringe plugged in the inlet. AFM experiments were performed at the SPM@ISMN microscopy facility in Bologna.

**SDS-PAGE analysis.** To desorb protein from carbon nanotubes, 50µl of dried carbon nanotubes were treated with 30µl of Laemmli buffer (Bio-Rad) in denaturating conditions. Also standard protein solutions were mixed with Laemmli buffer (Bio-Rad) in denaturating conditions and all samples were loaded onto a SDS-PAGE gel [59]. The gel was composed by a 4% polyacrylamide stacking gel (125 mM Tris–HCl, pH 6.8, 0.1%, m/v, SDS) and a 12% resolving polyacrylamide gel (in 375 mM Tris–HCl, pH 8.8, 0.1%, m/v, SDS buffer). A Tris-glycine buffer at pH 8.3 (with 0.1% SDS, m/v) was employed to fill the cathode, whereas a Tris buffer at pH 8.8 was used in the anode. Electrophoresis was performed in three steps with increasing voltage: first step was set at 50 V for 20 minutes, second step at 100 V for 40 minutes and third step at 150 V until the dye front reached the bottom of the gel. Staining and distaining were

performed with Colloidal Coomassie Blue and 7% (v/v) acetic acid in water, respectively[60].

**Mass spectrometry and data analysis.** Protein bands were excided to perform mass spectrometry analysis: they were subjected to washing steps with 50 mM Ammonium Bicarbonate (AmBic) and Acetonitrile (AcN), at 56 °C under stirring, in order to remove all colloidal Blue Coomassie. Afterwards, the gel slices were reduced and alkylated with 1.5 mg/ml DTT (in 50 mM AmBic) at 56 ºC and 10 mg/ml iodoacetamide (in 50 mM AmBic) at room temperature, respectively. Finally, proteins were digested with 0.02 µg/µl trypsin (in 25 mM AmBic) at 37 ºC overnight. The tryptic mixtures were acidified with formic acid (FA) up to a final concentration of 10% [61]. 8µl of tryptic digested sample were injected on a reversed-phase trap column (Acclaim PepMap100, C18, 100 Å, 5 µm, 100 µm ID x 2 cm length, Thermo Scientific) for peptide clean-up and pre-concentration. After clean-up, the trap column was placed in series with a fused silica reverse-phase column (picoFrit column, C18 HALO, 90 Å, 75 µm ID, 2.7 µm, 10.5 cm length, New Objective). A nano chromatography system (UltiMate 3000 RSLCnano System, Thermo Scientific) delivered a constant flow rate of 300 nl/min. The separating gradient ramped linearly from 4% buffer A (2% ACN and 0.1% FA in water) to 96% buffer B (2% water and 0.1% FA in ACN) in 60 min. The eluting peptides were on-line sprayed in a LTQ XL mass spectrometer (Thermo Scientific). Full mass spectra were acquired in the linear ion trap in the mass range *m/z* 350 to *m/z* 1800 Da. The 5 most intense ions were automatically selected and fragmented in the ion trap. Target ions already selected for fragmentation were dynamically excluded for 30 s. The MS data were analyzed by the Mascot search engine (Version 2.3.01), using the Proteome Discoverer software (v. 1.2.0 Thermo) and consulting specific UniProtKB/Swiss-Prot protein database (www.uniprot.org). In

detail, taxonomy *Equus Caballus* (31118 sequences, 15886002 residues) and *Bos Taurus* (50323 sequences, 21407192 residues) were selected for glutathione S-transferase and for carbonic anhydrase, respectively. Oxidation of methionine residues was set as variable modifications; one missed cleavages were allowed to trypsin; peptide mass tolerance was set to 1 Da, fragment mass tolerance to 0.8 Da, ion source cut-off of 20 and significance threshold of $p < 0.01$. MS data were performed both technical duplicates for each biological sample.

## 3. RESULTS AND DISCUSSION

### 3.1 DATABASE SCREENING.

The PDTD database [37] was screened to identify proteins able to recognize and bind to 1.3 nm diameter CNT. The strongly symmetric (10,10) CNT was used as representative of the 1.3 nm diameter family. PDTD is a web-accessible protein database for *in silico* target identification [41]. It is a structural database that contains 1207 entries, with structures taken from the Protein Data Bank (PDB), representative of the entire PDB. The top 100 proteins in the ranking obtained by screening the PDTD database are given in Table 1.

Given the limitations of the general procedure of the docking (i. e. the structures used in the virtual screening are crystallized conformations, approximations in the scoring functions ) and in the specific case of the docking between carbon nanotubes and proteins (i. e. protein unwrapping on hydrophobic surface of CNTs [50]), Table 1 does not want be a rigid ranking, but rather it represents a prioritization list to guide experiments. Proteins ranked by best binding energies should be considered as probable hits.

**TABLE 1.** Top 100 Protein Target Candidates for binding (10,10) CNT as ranked by the reverse docking procedure. The screening was carried out on 1207 protein structures.

| Rank | PDB | Protein Name | Rank | PDB | Protein Name |
|---|---|---|---|---|---|
| 1 | 1GTB | Glutathione S-transferase | 51 | 1JUE | Dihydroorotate Dehydrogenase |
| 2 | 1JVM | KcsA Potassium Channel | 52 | 1JMA | Herpes Simplex Virus Glycoprotein |
| 3 | 1IMB | Inositol Monophosphatase | 53 | 1OLS | Alpha Keto-Acid Reductase |
| 4 | 1ED5 | Nitric Oxide Synthase | 54 | 1QD6 | Phospolipase A |
| 5 | 1QE5 | Purine Nucleoside Phosphorylase | 55 | 1OZF | Acetolactate Synthase |
| 6 | 1JS6 | DOPA Decarboxylase | 56 | 1HP5 | Beta-N-Acethylhexosaminidase |
| 7 | 1EET | HIV-1 Reverse Transcriptase | 57 | 1DAR | Elongation Factor |
| 8 | 1HZX | Rhodopsin | 58 | 1I8D | Riboflavin Synthase |
| 9 | 1REQ | Methylmalonyl-COA Mutase | 59 | 2PLV | Poliovirus |
| 10 | 1QRD | Quinone Reductase | 60 | 1IJI | L-Histidinol Aminotransferase |
| 11 | 1H7X | Dihydropyrimidine Dehydrogenase | 61 | 1ITZ | Transketolase |
| 12 | 3PGK | Phosphoglycerate Kinase | 62 | 1PYY | Beta-Lactamases |
| 13 | 1W7L | Kynurenine Aminotransferase | 63 | 1BQS | MADCAM-1 Cell Adhesion molecule |
| 14 | 1MUO | Aurora-2 Serine-Threonine Kinase | 64 | 1QPB | Pyruvate Decarboxylase |
| 15 | 2ANH | Alkaline Phosphatase | 65 | 1K6W | Cytosine Deaminase |
| 16 | 1II5 | Glutamate Receptor | 66 | 1BYB | Soybean Beta-Amylase |
| 17 | 1DIH | Dihydrodipicolinate Reductase | 67 | 2G5T | Dipeptyl peptidase |
| 18 | 1WKQ | Cytidine Deaminase | 68 | 3HSC | ATP-ase fragment HeatShock Protein |
| 19 | 1V7M | Receptor binding Thrombopoietin AB | 69 | 1HT8 | Prostaglandin Synthase |
| 20 | 1KRA | Urease | 70 | 1C0N | Selenocysteine Lyase |
| 21 | 1ZT3 | Insulin like growth factor binding Protein 1 | 71 | 1I6O | Carbonic Anhydrase |
| 22 | 1DV1 | Biotin Carboxilase | 72 | 1E7W | Pteridine Reductase |
| 23 | 4FAB | Fab from autoantibody (BV04-01) | 73 | 1HV9 | N-Acetylglucosamine-1-PO(4) Uridyltransferase |
| 24 | 1XFH | Glutamate Transporter | 74 | 2A3L | Adenosine-5-Monophosphate Deaminase |
| 25 | 2DDH | Acyl-CoA Oxidase II | 75 | 1EVZ | Glycerol 3-phosphate dehydrogenase |
| 26 | 1SFT | Alanine Racemase | 76 | 1ZSX | Human $K^+$Channel Kv Beta-subunit |
| 27 | 1DGD | Dialkylglycine Decarboxilase | 77 | 1GAI | Gluco-amylase |
| 28 | 1PQ2 | Cytochrome P450 | 78 | 1Y5M | 11-β-hydroxysteroid Dehydrogenase |
| 29 | 1AG8 | Aldehyde Deydrogenase | 79 | 1FIE | Human Coagulation Factor |
| 30 | 1GPU | Transketolase | 80 | 2F2S | Acetoacetyl-Coa Thiolase |
| 31 | 1OVM | Indolepyrovate Decarboxylase | 81 | 1HES | Mu2 Adaptin Subunit |
| 32 | 1TDB | Thymidylate Synthase | 82 | 1UKZ | Uridylate Kinase |
| 33 | 2YHX | Hexokinase B | 83 | 1TYP | Trypanothione Reductase |
| 34 | 2CBI | Glycoside Hydrolase | 84 | 1HN4 | Phospholipase A2 |
| 35 | 1OVD | Dihydroorotate Dehydrogenase | 85 | 3CLA | Chloramphenicol Acetyl-Transferase |
| 36 | 1E5F | Methionine Gamma-Lyase | 86 | 1DVS | Transthyretin |
| 37 | 1W6G | Amine Oxidase | 87 | 1OSZ | MHC Class I H-2kb Heavy Chain |
| 38 | 1W07 | Acyl-CoA Oxidase I | 88 | 1MDR | Mandelate Racemase |
| 39 | 1Q44 | Steroid Sulfotransferase | 89 | 1JR1 | Inosine Monophosphate Deydrogenase |
| 40 | 1DBK | Anti-progesterone Antibody | 90 | 1N9E | Lysyl Oxidase |
| 41 | 1I9Z | Inositol Polyphosphate 5-Phospatase | 91 | 1P8V | Platelet Receptor Glycoprotein |
| 42 | 2AYO | Ubiquitin protease | 92 | 1HHI | Peptides presented by HLA-A2 |
| 43 | 2HHA | Dipeptyl peptidase | 93 | 1P93 | Glucocorticoid Receptor |
| 44 | 1EFR | F1-ATPase | 94 | 2LGS | Glutamine Synthetase |

| | | | | | |
|---|---|---|---|---|---|
| 45 | 1LBV | Inositol,Fructose 1,6 biposphate/ase | 95 | 1WUR | GTP Cyclohydrolase |
| 46 | 1O4S | Aspartate Aminotransferase | 96 | 1A3G | Amino Acid Aminotransferase |
| 47 | 1NEK | Succinate Dehydrogenase | 97 | 1QKT | Estrogen Nuclear Receptor |
| 48 | 1PPI | Alpha-Amylase | 98 | 1IGJ | 26-10 FAB:Digoxin |
| 49 | 1FI2 | Oxalate Oxidase | 99 | 1YTZ | Skeletal Muscle Troponin |
| 50 | 1JOA | NADH-Peroxidase | 100 | 1XUP | Glycerol Kinase |

## 3.2 EXPERIMENTAL VALIDATION OF THE PROTOCOL

In the top 100 protein candidates, there are three proteins that experimentally have already demonstrated interactions with CNTs: KcsA potassium channel [62], rhodopsin [63] and cytochrome P450 [64]. Since the procedure was blind, this finding represents a first step to validate the prediction ability of the protocol. To further validate the procedure, we tested the ability of some identified proteins to bind and disperse in water CNTs.

**Dispersion of CNTs by proteins.**

The most straightforward application to further validate the procedure is to test the ability of some selected proteins from Table 1 to bind and disperse in water CNTs. Formation of stable dispersions of debundled nanotubes is one of the most important prerequisites for the technological exploitation of CNTs. Chemical functionalization of the CNT surface [65,66], or noncovalent approaches [66–68] are used to obtain debundled nanotubes. The noncovalent approaches are the most attractive because they are able to disperse CNTs in water, while preserving the properties of CNTs [69]. Amphiphilic molecules, surfactants, synthetic polymers, biopolymers, DNA, and short peptides have been used to disperse CNTs [67,68]. In recent years, also proteins have become widely used as CNT-dispersing agents [8,70–77] because they can be considered as naturally amphiphilic biopolymers. Taking advantage of this feature, the use of proteins as dispersant agents may avoid complicated synthetic procedures or the use of organic solvents.

Martin and coworkers defined a set of general features that must be shared by host molecules to recognize efficiently carbon nanoparticles for their dispersion in water or in organic solvents [78,79]:

i) The presence of a nonpolar cavity of the appropriate size to fit the carbon nanoparticle [78,79],

ii) Concave–convex complementarity [78,79] should be at the basis of the recognition process,

iii) An high degree of preorganization of the host will lower the entropic cost for guest binding [78,79].

Most or all proteins offer these three features. In particular, evolution endowed them with

i) non polar cavities or crevices, rich in aromatic aminoacids,

ii) recognition abilities based on shape complementarity,

iii) high level of host preorganization due to their 3D structure.

From Table S1, we selected the first protein of the rank, namely glutathione S-transferase, and the three proteins that are commercially available at low cost. They are hexokinase (rank 33), amylase (rank 48) and carbonic anhydrase (rank 71).

The CNTs were ultrasonicated in aqueous solution of the proteins, the solution was centrifuged and finally the surnatant was collected. This resulted in highly dispersed and debundled CNTs in the aqueous system. A picture of vials containing the debundled CNTs from the different proteins is shown in the inset of Figure 1. The different colors correspond to the amount of CNTs in the solutions.

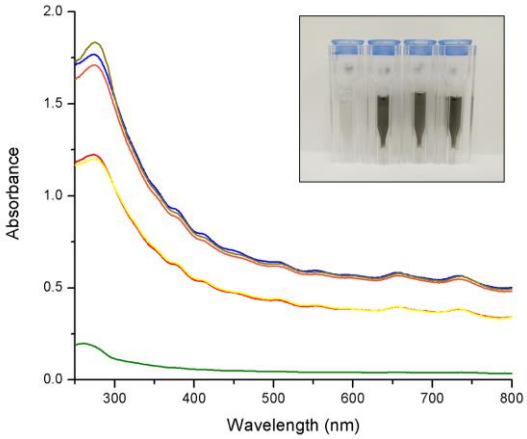


**Figure 1.** UV-vis absorbance spectra of the hybrids: glutathione S-transferase-CNT (cyan), lysozyme-CNT (brown), carbonic anhydrase-CNT (orange), hexokinase-CNT (red), bovine serum albumin-CNT (yellow), α-amylase-CNT (green). Inset: Cuvettes containing the dispersed CNTs obtained from the selected proteins. From left: α-amylase, hexokinase, carbonic anhydrase, and glutathione S-transferase.

The UV-vis spectra showed that the best performances are obtained by glutathione S-transferase and carbonic anhydrase that work as well as the gold-standard for CNT dispersion, namely lysozyme. The dispersion obtained by hexokinase is similar to that obtained by bovine serum albumin, another protein very commonly used to disperse CNTs. The performance of α-amylase is the lowest. The behavior of α-amylase is however due, not to a poor prediction, but to the low solubility of this protein in water. From figure 1 it also appears that the UV-vis spectra of the protein-CNTs hybrids show well-resolved peaks. The peak at 280 nm is due to the proteins, caused by the absorption of aromatic amino acids. The peaks from 440 to 600 nm are attributed to the first van Hove transitions of metallic-CNTs ($M_{11}$), while the peaks from 550 to 800 nm are attributed to the second van Hove transitions of semimetallic-CNTs ($S_{22}$). This mean that the selected proteins are able to disperse both metallic and semiconducting CNTs

of 1.3 nm of diameter [80]. It is well established that only debundled CNTs exhibit well-defined peaks in the visible region due to the van Hove transitions [80].

Atomic force microscopy (AFM) images of the protein-CNTs hybrids (Figure 2) confirm that during sonication, the CNTs were debundled due to the strong interactions of the proteins with the CNTs surface, which resulted in highly dispersed protein-nanotube adducts in the aqueous systems.

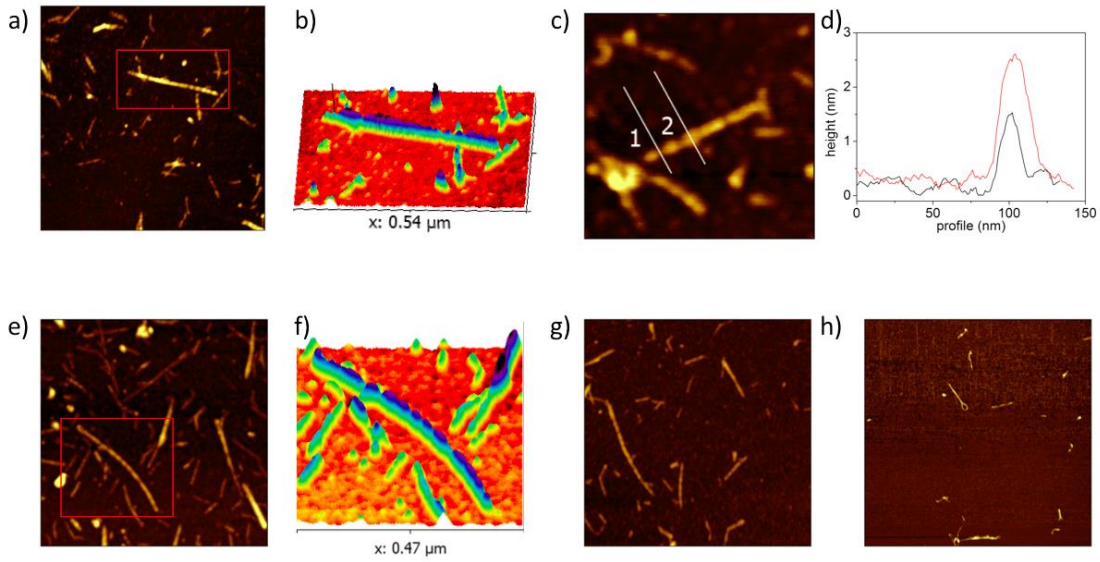


**Figure 2.** AFM images of proteins-CNT hybrids. Glutathione S-transferase-CNT: a) top view (1µm x 1µm); b) 3D rendering of the rectangular selection indicated in figure 2a, c) magnification, top view (0.3µm x 0.3µm); d) profile analysis: profile 1, in figure 2c (black line), profile 2, in figure 2c (red line). Hexokinase-CNT: e) top view (1µm x 1µm); f) 3D rendering of the rectangular selection indicated in figure 2e; g) carbonic anhydrase-CNT, top view (1µm x 1µm); h) α-amylase-CNT, top view (5µm x 5µm).

The profile analysis of glutathione S-transferase-CNT (Figures 2c,2d), clearly shows the dispersion of 1.3 nm diameter $CNT_S$ (black line in figure 2d, profile 1 in figure 2c), and the protein surrounding the tube (red line in figure 2d, profile 2 in figure 2c).

In the magnification of Figures 2b,2f, it is possible recognize the proteins astride on the CNTs. Even if the quantitative yield of dispersion is low for α-amylase (figure 2d), it appears that the qualitative behavior is similar to the other proteins, with well-dispersed tubes (see Figure S1). To eliminate the possible surface effects due to the adsorption of proteins on the surface in the dried state, for the Glutathione S-transferase-CNT hybrid the AFM analysis is repeated also in liquid (Figure S2). Even if the image has a lower resolution due to the slight drift of the objects in the hydrated state, the topology is the same, showing in addition a more realistic dimension of the proteins, that in this condition remain hydrated.

All hybrids were highly stable in the aqueous system; no traces of precipitation were observed even after three months under ambient conditions.

Following a recently optimized procedure to study CNT-protein interactions [59], samples of proteins-CNTs adducts were analysed by sodium dodecyl sulphate-polyacrylamide gel electrophoresis (SDS-PAGE) and mass-spectometry to confirm the interaction of the proteins with CNTs. The most performing proteins: glutathione S-transferase-CNT and carbonic anhydrase-CNT were selected for this study.

Proteins were desorbed from protein-CNT adducts treating the dried sample with Laemmli buffer in denaturating conditions. The same procedure was used also for standard protein solutions and all samples were loaded onto a SDS-PAGE gel (Figure 3).

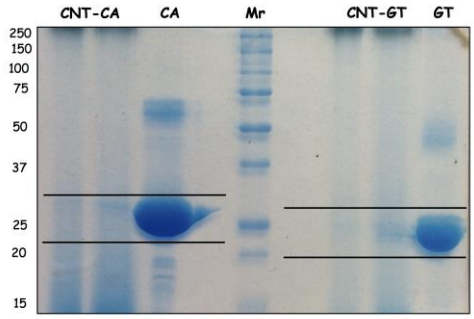


**Figure 3.** Coomassie Blue stained SDS-PAGE gels corresponding to carbonic anhydrase-CNT (CNT-CA), carbonic anhydrase (CA), glutathione S-transferase-CNT (CNT-GT) and glutathione S-transferase (CNT-GT) eluates.

Figure 3 depicted the SDS-PAGE profiles of control proteins and of the carbonic anhydrase and glutathione S-transferase eluates from proteins-CNT adduct. The lanes have showed the same bands, referred to the control proteins. Protein bands were excided to perform mass spectrometry analysis. The proteins were identified by tryptic fingerprinting and mass spectrometry as showed in Table 2 and Table S1 (list of all the peptides identified in the samples) confirming their interaction with the CNTs.

**Table 2.** List of proteins (accession number, name, mascot score, molecular weight, number of peptides) identified in SDS-PAGE slices.

| SDS-PAGE Slice | Accession Number | Protein Name | Mascot Score | Mr | N° peptides |
|---|---|---|---|---|---|
| | | | | | |
| GT | M9ZUR8 | Glutathione S-transferase A1 OS=Equus caballus OX=9796 GN=GSTA1 PE=2 SV=1 | 8119 | 25676 | 13 |
| CNT-GT | M9ZUR8 | Glutathione S-transferase A1 OS=Equus caballus OX=9796 GN=GSTA1 PE=2 SV=1 | 6001 | 25676 | 19 |
| | | | | | |
| CA | P00921 | Carbonic anhydrase 2 OS=Bos taurus OX=9913 GN=CA2 PE=1 SV=3 | 9040 | 29096 | 16 |
| CA | F1N0H3 | Carbonic anhydrase 2 OS=Bos taurus OX=9913 GN=CA2 PE=1 SV=2 | 7152 | 27733 | 14 |
| CNT-CA | P00921 | Carbonic anhydrase 2 OS=Bos taurus OX=9913 GN=CA2 PE=1 SV=3 | 5670 | 29096 | 23 |
| CNT-CA | F1N0H3 | Carbonic anhydrase 2 OS=Bos taurus OX=9913 GN=CA2 PE=1 SV=2 | 5188 | 27733 | 22 |

Figure 4 shows the recognition process between the four proteins and CNTs, with 1.3 nm of diameter. It is evident the surface complementarity between the proteins and the

CNT surface, identified by the virtual screening procedure. Prediction and experiments well matched each other.

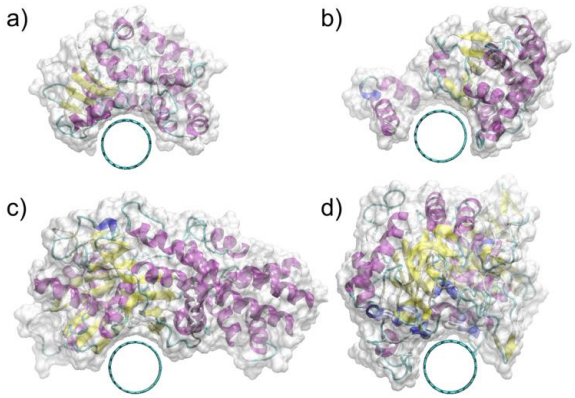


**Figure 4.** Interaction between a) glutathione S-transferase; b) carbonic anhydrase, c) hexokinase; d) α-amylase and a CNT of 1.3 nm of diameter. In cartoon the secondary structure of the protein, in transparent white the surface representation of the protein.

For the four CNT-protein hybrids tested here, a MM-GBSA analysis [42,43] of the structures in their minimized geometries provides a quantitative description of the CNT-binding pocket and identifies the most effectively interacting residues in order to provide general rules for the optimization of the binding pocket of proteins to accommodate CNT. Table 3 shows the 10 largest interactions between the proteins and the CNT.

**TABLE 3.** Interaction energies (kcal $mol^{-1}$) of the top 10 residues interacting with the CNT of 1.3 nm of diameter.

| | | | | | |
|---|---|---|---|---|---|
| Glutathione S-transferase | Tyr 111 = -12.5 | Tyr 104 = -11.9 | Met 94 = -11.0 | Phe 52 = -10.2 | Leu 100 = -7.1 |
| | Met 69 = -6.8 | Trp 8 = -6.3 | Ser 93 = -6.1 | Gln 67 = -5.8 | Arg 42 = -5.7 |
| Carbonic anhydrase | Tyr 83 = -11.5 | Ile 116 = -8.4 | Leu 113 = -8.3 | Phe 61 = -8.2 | Ile 4 = -8.0 |
| | His 63 = -7.6 | Leu 115 = -6.9 | Leu 88 = -6.4 | Asn 76 = -5.8 | Leu 7 = -5.2 |
| Hexokinase | Phe 105 = -8.7 | Thr 222 = -8.3 | Pro 455 = -7.7 | Val 454 = -6.2 | Lys 111 = -6.1 |
| | Asp 223 = -5.4 | Asp 447 = -5.2 | Thr 107 = -5.1 | Gln 109 = -5.1 | Asp 448 = -5.0 |

| | | | | | |
|---|---|---|---|---|---|
| α-amylase | Tyr 151 = -12.4 | Leu 237 = -7.2 | Val 163 = -6.9 | Glu 149 = -5.9 | His 305 = -5.1 |
| | Trp 269 = -4.4 | Glu 240 = -4.4 | Ser 310 = -4.3 | Ser 150 = -4.1 | Ser 145 = -4.0 |

In practice, these interactions allow to identify quantitatively the "CNT binding propensity" of the residues constituting the binding pocket. From Table 1 it is clear that proteins are able to establish a large number of interactions with CNTs that include:

i) *$\pi$-$\pi$ stacking interactions* that can be established between aromatic residues (tyrosine, phenylalanine, tryptophan, histidine) and the CNT surface [1–7,81].

*ii) Hydrophobic interactions* that can be established in water between aliphatic residues and the CNTs surface. The hydrophobic interactions remove ordered water molecules from the vicinity of a non-polar region. The hydrophobic residues cluster together to avoid exposure to water. The interaction energy increases at the increasing of the exposed hydrophobic surface (methionine, leucine, isoleucine, valine) [1–7].

iii) *Surfactant-like interactions* where the amphiphilic residues can behave similarly to surfactants and solvate CNTs. The hydrophobic aliphatic chains of these residues interact with the CNT tube surface, whereas the hydrophilic groups point out toward water (serine, threonine, glutamine, asparagine, arginine, lysine, aspartate, glutamate) [1–7].

## 3.3 DESIGN OF FUNCTIONAL MATERIALS AND NEW APPLICATIONS OF THE PROTEINS-CNT HYBRIDS.

After the validation of the identification protocol, we carried out a detailed analysis of the results aimed at suggesting possible technological application for the protein/CNT hybrids identified by the procedure. The top 100 strongly binding proteins constitute a good protein targets for practical applications.

Many identified proteins are membrane proteins. These proteins are expected to strongly interact with hydrophobic CNT surface since they have the regions optimized for interactions with the hydrophobic part of membrane. In case of technological applications of these membrane-bound proteins it is important to be aware of the difficulties in their handling and manipulations.

**Sorting CNTs of different diameters.** Protein can be used to recognize different-diameter CNT's [50,74,82,83]. Proteins can be used as supramolecular hosts to interact specifically with CNT of different sizes. In Table 1 there appear tweezer-like and cyclic like proteins that bind to CNT. The tweezer-like troponin (PDB=1YTZ) and the cyclic-like cytidine deaminase (PDB=1WKQ) (Figure 5) are able to recognize selectively specific CNT-diameters and can be used for diameter-based CNTs sorting.

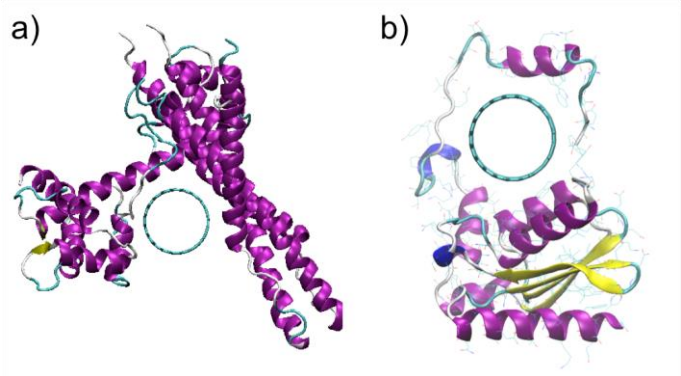


**Figure 5.** a) Tweezer-like interaction between troponin and (10,10) CNT; b) Recognition between the cyclic structure of cytidine deaminase and (10,10) CNT.

**CNTs as a support for enzyme immobilization.** CNTs can support enzymes [50,84]. The protein/CNT hybrids show a high, or even increased, biological activity, stability, and reusability [50,84]. The conjugates perform well even in strongly denaturing environments such as high temperatures or in organic solvents and improve the results obtained on conventional flat supports [84]. As an example, multicomponent fibers that

include single-walled carbon nanotubes and lysozyme were reported [85]. These fibers exhibit antibacterial and mechanical properties that make them suitable for fabrics, clothing and technical textiles in medical environments. Upon adsorption, lysozyme remains active [86].

Practical applications of enzymes adsorbed on the surface of (10,10) CNTs are readily suggested by an analysis of Table 1. Urease, a nickel-dependent metalloenzyme, catalyzes the hydrolysis of urea to form ammonia and carbon dioxide. Its immobilized form has found broad applications, such as blood detoxification in artificial kidneys, removal of urea from beverages and foods in food industry, and reduction of urea content in effluent treatment in agriculture. CNTs may represent an optimal platform for non-covalent immobilization of urease (PDB=1KRA), considering that the active site of the protein is located away from the interaction area of the protein with the CNT (Figure 6).

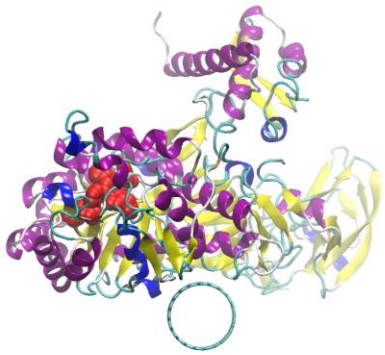

**Figure 6.** Interaction between (10,10) CNT and urease. In red are the catalytic residues of the proteins. Other very interesting proteins can be used to create hybrids, as CNT/amylases (PDB = 1PP1, PDB = 1BYB, PDB = 1GAI) or CNT/carbonic anhydrase (PDB = 1I6O), with potential technology exploitation.

**Ordered assemblies of hierarchical objects containing CNTs and proteins.** Nano-manipulation is a promising approach to obtain complex nano-assemblies. Protein

junctions are one of the constitutional elements of such assemblies and can be used to integrate nanoscale objects in an ordered and hierarchical manner. Both surface recognition regions and favorable inter-protein packing interactions can be designed to govern the final assembly. β-barrel proteins are robust and flexible components in nanotechnology [87] and can guide the assembly of nanotubes. In Figure 7, Phospholipase A1 (PDB=1QD6) can interact with (10,10) CNT (Fig. 7a) and act as a spacer for the assembly of two nanotube (Fig. 7b). It can act as a railroad tie, able to organize the tubes as rails. The ability of β-barrel proteins to dimerize (Fig. 7b) or the use of β-barrel proteins of different sizes (Fig. 7c) can tune the protein/CNT assembly.

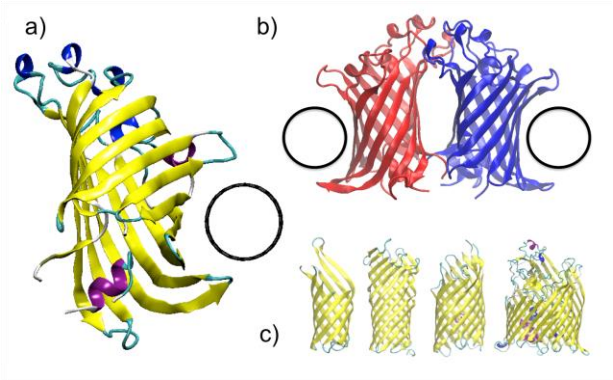


**Figure 7.** a) Interaction between (10,10) CNT and phospholipase A1; b) Dimeric structure of Phospolipase A1, c) β-barrel proteins of different dimensions, from the left: 8 β-strand OmpA, 10 β-strand OmpT, 12 β-strand EsoO, 22 β-strand FhuA.

**CNTs as protein carriers for vaccines.**

CNTs show features that can make them scaffolds for vaccine compositions [88–91]. The noteworthy properties of vaccines that use CNTs as carriers include stability *in vivo*, minimal cytotoxicity and the ability to present peptides attached to the carrier surface with the correct conformation for recognition, without perturbing the secondary

and tertiary structure. In addition, CNT-viral protein complexes are capable of generating specific immune responses [88–91]. CNTs can therefore be exploited as carriers to administer vaccines boosting the efficacy of antigens that cannot induce a sufficient and suitable response. However, although recent work has demonstrated the potential of CNTs to amplify the immune response as adjuvants, other results have also linked their proinflammatory properties to harmful health effects.

In the ranking of Table 1, it appears that (10,10) CNT can be used to support *herpes simplex* virus (HSV) glycoprotein (PDB=1JMA) or capsid protein poliovirus (PDB=2PLV). HSV glycoprotein D (gD) is one of the most important viral immunogens, which has an essential role in virus infectivity and induction of immune responses. (10,10) CNT can support this viral protein (Figure 8a) leaving intact the immunogenic site (in Figure 8b the possible recognition with the ectodomain of its cellular receptor HveA).

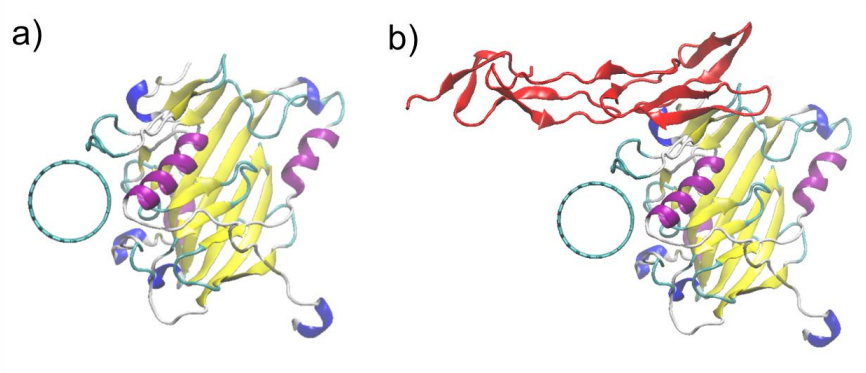


**Figure 8.** a) Interaction between (10,10) CNT and the truncated ectodomain of gD; b) Interaction between the hybrid (10,10) CNT/truncated ectodomain of gD with the ectodomain of its cellular receptor HveA (in red). The (10,10) CNT can also be used as a support for the binding of human leukocyte antigen (PDN = 1HHI) that is commonly used for immunization to presents short polypeptides to the immune system.

**Protein/CNT hybrids as substrates for cell growth**. CNTs functionalized with fibronectin or collagen, which are extracellular matrix proteins, are effective platforms to control cell adhesion [92]. Mucosal addressin cell adhesion molecule 1 (MAdCAM-1) is expressed on the endothelium in mucosa. Cell adhesion molecules (CAMs) are proteins located on the cell surface that are involved in binding with other cells or with the extracellular matrix (ECM) in the process called cell adhesion. MAdCAM-1 guides the specific homing of lymphocytes into mucosal tissues [93]. MAdCAM-1 (PDB=1BQS) is identified as a (10,10) CNT binding protein. The structure of MAdCAM-1 revealed two separate integrin-recognition motifs [93]. After binding to CNT both regions remain exposed (Figure 9), which may lead to a functional assembly able to guide the growth of cells over the CNT surface.

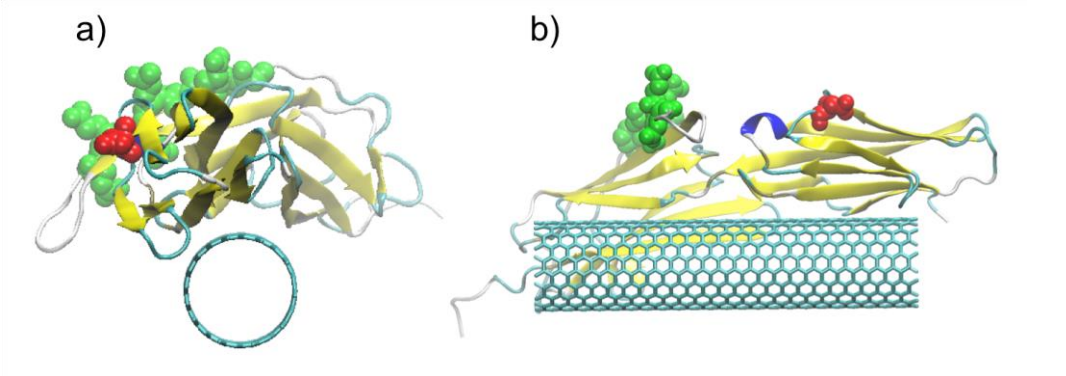


**Figure 9.** Interaction between (10,10) CNT and MAdCAM-1, a) front view, b) side view. The two integrin recognition motifs are showed: in red, the key integrin binding residue, Asp42, that resides in the CD loop of domain 1; in green, the second binding site associated with an unusually long D strand in domain 2. Other interesting targets identified are platelet membrane glycoproteins (PDB= 1P8V). These glycoproteins are engaged in platelet adhesion to the extracellular matrix and can be used efficiently in regenerative medicine.

**Protein/CNT hybrids as carriers for therapeutic and imaging materials.** CNTs can load in their hollow interior a variety of cargoes, including pharmaceutically relevant agents and/or materials of medical imaging [94–97]. CNTs can be used for the intracellular delivery of a therapeutic enzyme [98]. Protein functionalized CNT shows an improved vectorization ability if compared to pristine CNTs [99]. CNT constructs for tumor-cell targeting were synthesized by coating CNTs with monoclonal antibodies, with the intent of delivering CNTs selectively to specific cellular sites [100–102].

Transthyretin that appears in Table 1, was proposed as an innovative transporter for nanoparticles across blood–brain barrier by receptor-mediated transcytosis [103]. Transthyretin (PDB=1DVS)/(10,10)CNT hybrids (Figure 10) may introduce a revolutionary way to improve BBB penetration of CNTs.

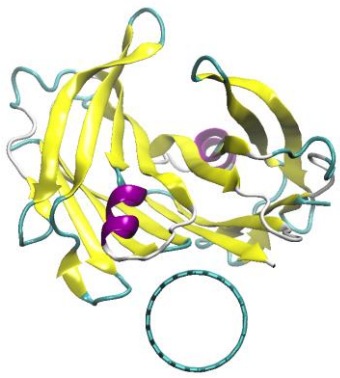

**Figure 10.** Interaction between (10,10) CNT and transthyretin.

**Protein coating of CNTs to make them biocompatible.**

The interaction between proteins and CNTs, i.e. the formation of CNT-protein corona, plays a crucial role in determining the biological effects of CNTs. Once injected in a physiological environment, CNTs interact with biological components and are surrounded by a protein corona. The formation of bio-corona, due to adsorption of biomolecules onto CNTs surface in a physiological environment, may lead to a

modified biological "identity" of CNTs, contributing to determine their biocompatibility and toxicity[59].

Experimentally the binding of blood proteins such as fibrinogen, immunoglobulin, albumin, transferrin, and ferritin, to carbon nanotubes reduces CNT cytotoxicity [104,105]. The binding to a plasma protein can “hide” any uncovered area of a carbon nanotube. It can also prevent filtration and expulsion by the kidneys (reduction of the clearance) and extend its plasma half-life (longer retention time).

Factor XIII is an interesting protein for coating carbon nanotubes because it has a long half-life, ranging from 5 to 9 days, and is present naturally in the plasma since it is an enzyme involved in the blood coagulation system. In Figure 11 the interaction of the Factor XIII (PDB=1FIE) with (10,10) CNT is shown.

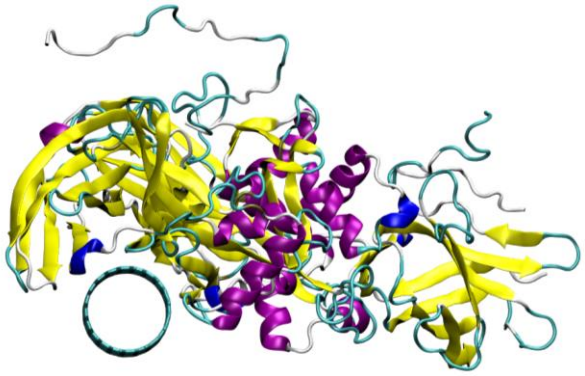

**Figure 11.** Interaction between (10,10) CNT and Factor XIII.

Adsorption of proteins onto CNTs alters the toxicological profile of CNTs, modifying cellular responses and other biological effects. The formation of a well-defined CNT-protein corona, may control cellular trafficking and systemic translocation of the CNTs in the body.

**CNTs as pharmaceutical scaffolds for protein inhibition.** CNT-based ligands can serve as effective inhibitors [64] and, over conventional inhibitors, have some advantages because of their geometrical and chemical properties. The geometry of CNTs is expected to complement the binding pockets of different proteins (in particular crevices). Inositol monophosphatase (PDB = 1IMB) and nitric oxide synthase (PDB = 1ED5) are well known therapeutic targets. Another interesting target is HIV-1 reverse transcriptase (PDB=1EET). Since CNTs were previously suggested to inhibit also HIV-1 protease [106] and HIV-1 integrase [107], the discovery of this new target may represent the basis for a new multitargetted HIV therapy based on a carbon nanotubes scaffolds. In fact, the tubular structure of CNTs is able to occupy the DNA/RNA binding pocket of the HIV-1 reverse transcriptase (Figure 12). Very recent work suggested the antiviral potentiality of dispersible CNTs and proved their *in vitro* ability to interact with viral enzymes and to act as HIV inhibitors [108].

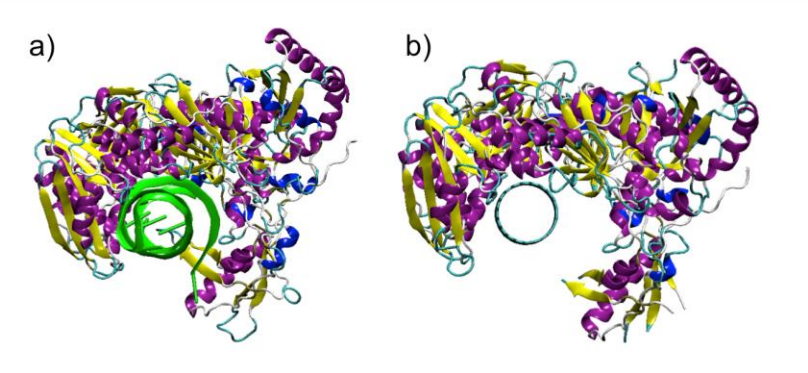


**Figure 12.** a) Interaction between HIV-1 reverse transcriptase and DNA/RNA (in green) and b) Interaction between HIV-1 reverse transcriptase and (10,10) CNT.

The commensurability between CNTs and the nucleic acid double helix, may also suggest the design of CNTs derivatives able to interfere with the proteins involved in the interaction with DNA/RNA.

**Nano-toxicology of CNTs.** CNTs may also interfere directly with biological functions of proteins. The toxicological profile of CNTs is still emerging [109]. The protocol used in the present paper can suggest targets and mechanisms by which proteins interact with carbon nanomaterials, explaining both biological and toxicological effects. Park et al. reported that CNTs block ion channel proteins [62]. They speculated that nanotubes fit into the pore and hinder ion movement. In this mechanism CNTs should remain completely exposed to water.

In the case of the ion channel blocker, our approach suggests a different mechanism. In the complex, the hydrophobic CNTs is immersed in the hydrophobic region of the cellular membrane and interacts with the helices of the channel (PDB=1JVM).

The role of the CNT is to hamper the conformational changes requested for the passage of the ions in the channel (Figure 13). It therefore "blocks the gearbox" that opens and closes the voltage-gated potassium channel.

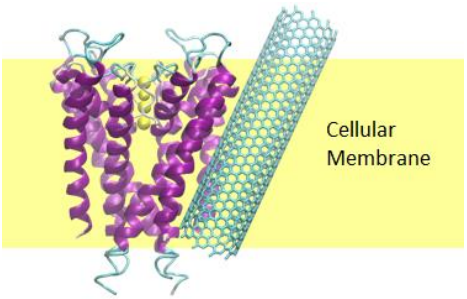


**Figure 13.** Interaction between $K^+$ Channel and (10,10) CNT.

This mechanism is also in agreement with recent data about the membrane transport of CNTs, able to penetrate the membrane as a needle [110–112].

Very recently CNTs have appeared to inhibit the cytochrome P450 enzyme [64] (PDB = 1PQ2) and molecular dynamics simulations suggested that inhibition of the catalytic activity of the enzyme is mainly caused by the blocking of the exit channel for

substrates/products [64]. This is the mechanism suggested independently by our docking prediction.

**Protein/CNT hybrids for bioelectronics, biosensing and biofuel cells.** CNTs can be used to link proteins identified in Table 1 to electrodes and use the systems as enzyme microelectrodes for biosensors or biofuel cell applications [113]. Quinone reductase (PDB= 1QRD), acyl-CoA oxidase (PDB = 2DDH, PDB = 1W07), aldehyde dehydrogenase (PDB = 1AG8), transketolase (PDB = 1GPU, PDB = 1ITZ), succinate dehydrogenase (PDB = 1NEK), oxalate oxidase (PDB = 1FI2) are some of such proteins. Heme proteins have already been electrochemically contacted with CNTs to produce biosensor [114]. The CNTs can assist electron transfer to the electrode [34,114], orient the protein, and provide efficient, reproducible electrical conduction [114].

In this area the highest-ranking protein is quinone reductase. Quinone reductase is a homodimeric FAD-containing enzyme that catalyzes obligatory NAD(P)H-dependent two-electron reductions of quinones. All the prosthetic groups involved in the electron/hydride transfers from NAD(P)H to FAD and from FADH2 to the quinone are not perturbed by the presence of the CNT (Figure 14) that, on the contrary, may promote the electron transfer from the protein to the electrode [114].

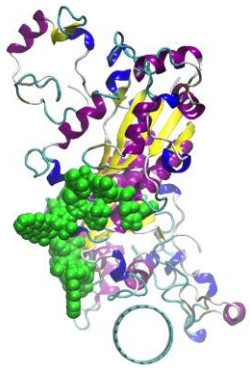

**Figure 14.** Wiring-up quinone reductase to electrodes by CNT. In green, the prosthetic groups involved in the electron/hydride transfers: NAD(P)H, FAD, FADH2, quinone.

**Protein functionalized carbon nanotube for Field Effect Transistors (CNT-FET)**

Semiconducting CNTs have been used to fabricate field-effect transistors (FETs) [115]. The conductivity of CNTs is sensitive to the environment. It therefore varies in the presence of charges and/or dipoles of adsorbed molecules [116]. In CNT-FET sensors the active detection area is downscalable to the size of individual proteins. They are characterized by high sensitivity because the whole current passes through the detection point [117]. CNT-FETs can also detect bio-recognition events. In the case of biotin-streptavidin binding, for example [118], the source-drain current dependence on gate voltage of the CNT-FET showed a significant change upon streptavidin binding to the biotin-functionalized carbon nanotube [118]. The use of functionalized CNT-FETs can be extended also to antigen-antibody or virus recognition. In practice, CNT-FETs eavesdrop on what proteins do and convert the information of the binding into an electric signal. Many proteins that appear in table 1 can be used to create functionalized CNT-FETs able to recognize important clinical targets. The most important example is probably the antigen-binding fragment of the anti-digoxin monoclonal antibody 26-10 (PDB=1IGJ), Figure 15. Only semiconducting CNTs can be used in FETs due to their intrinsic bandgaps: semiconducting CNTs of diameter 1.3 nm for potential use in FET can be (10,9), (12,7), (13,6), (15,4), (16,2), (16,3), (11,9), (12,8), (17,0), (17,1) CNTs.

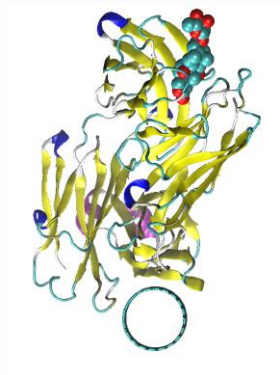

**Figure 15.** Interaction between 1.3 nm CNT and the antigen-binding fragment of the anti-digoxin monoclonal antibody 26-10.

Digoxin inhibits the $Na^+$,$K^+$-ATPase and is used in the treatment of congestive heart failure. Digoxin has only a small therapeutic range of concentrations (0.5/2.0 ng $mL^{-1}$) and its use requires its strict monitoring in the blood levels to minimize toxicity. Sensing serum digoxin levels is crucial because it is necessary to monitor constantly the serum digoxin levels of patients under treatment, as a guide to therapy and to treat otherwise fatal digoxin intoxication. Functionalized CNT-FETs with anti-digoxin antibodies can allow the development of highly sensitive, label-free, cost-effective, simple and disposable sensors able to sense real-time serum digoxin levels. Other interesting hybrids for clinical sensing can be developed using CNTs hybrids obtained bio-conjugating glutamate receptor (PDB = 1II5), anti-progesterone antibody (PDB = 1DB4), glucocorticoid receptor (PDB = 1P93) and estrogen nuclear receptor (PDB = 1QKT) with the nanotubes.

**Protein/CNTs hybrids for the development of biomolecular nanodevices**

Owing to their well-defined geometry, exceptional mechanical properties, and extraordinary electrical characteristics, CNTS may serve as building blocks for complex structures, tools, sensors, and actuators [119,120]. Rhodopsin (PDB=1HZX) is an example of a protein commonly used as a bio-nano component [121]. It is naturally found in biological systems as light sensors. It can also be used in collectors of solar energy. The direct electron communication between CNTs and rhodopsin (Figure 16) can be exploited for effectively interfacing the transport properties of CNTs with the photoactivity of the protein for new photoconversion applications in photovoltaic devices [121].

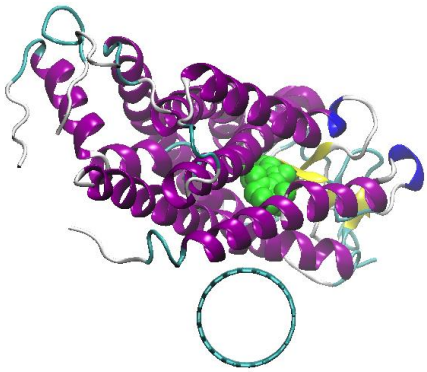

**Figure 16.** Interaction between (10,10) CNT and rhodopsin, in green, the prosthetic group chromophore, 11-cis-retinal.

CNTs can also be used as fundamental components for molecular-level robots and nanomachines [119]. Microtubules are responsible for a variety of cell movements. The shape, size and physical property of CNTs also parallel the structural and physical properties of intracellular microtubules, despite remarkable differences in their chemical compositions. Indeed, both microtubules (MTs) and CNTs are hollow cylindrical structures. The hollow cylinder in MTs is formed by packing protein into a helical lattice, while a hexagonal lattice of carbon atoms defines the cylindrical structure in CNTs. Proteins that interact with MT are potentially able to interact with CNTs as discussed previously in the case of skeletal muscle troponin/CNTs hybrids (Figure 5a), and can be used to create new generation of linear nanomotors.

## 4. CONCLUSION

To date, the prediction of stable protein/CNTs adducts has received only conjectural answers. Here a protein database is systematically screened with the purpose of identifying selectively and ranking proteins for their ability to bind with 1.3 nm diameter CNTs. The propensity to form CNTs/protein hybrids is ranked.

The procedure effectively identifies as high scorers proteins that have been reported to form CNT/protein hybrids.

The highest scoring protein and three other proteins –selected for their low cost– were experimentally tested for binding to CNTs and found to form stable adducts.

The interaction was confirmed by AFM measurements and SDS-PAGE followed by mass-spectrometry.

The hybrids with the highest scoring are also evidenced and discussed for a variety of practical applications that cover, sorting of CNTs of different diameters by proteins, CNTs as a support for enzyme immobilization, ordered assemblies of hierarchical objects containing CNTs and proteins, CNTs as protein carriers for vaccines, protein/CNT hybrids as substrates for cell growth and cell interfacing applications, protein/CNT hybrids as targeted carriers for therapeutic and imaging materials, protein coating of CNTs to make them biocompatible, CNTs as pharmaceutical scaffolds for protein inhibition, nano-toxicology of CNTs, protein/CNT hybrids for bioelectronics, biosensing and biofuel cells, protein functionalized carbon nanotube for field effect transistors, protein/CNTs hybrids for the development of biomolecular nanodevices. In the paper:

1) the approach is validated on the basis of new experimental data obtained here

2) The best protein for every application is identified by the reverse docking procedure.

3) The "fingerprint analysis" (provided by MM-PBSA calculations) identified i) the amino acid residue with the greater tendency to bind CNTs, ii) the hot and weak spots in the binding between the proteins and CNTs, determining quantitatively for every protein residue their role in the binding.

~~The approach can be extended to CNTs of different diameters.~~

Understanding the interactions at the nanobio interface is only the first step for the safe use of nanotechnology and for the design of nano materials for biological applications [122–125]. Engineering specific interactions between proteins and CNTs will allow further developments of the proposed applications.

The design of chemical functionalization on the tube surface [126], or protein engineering [127] to create protein mutants, will make possible a) the improvement of the binding (positive mutations) conserving the hot spots, and mutating the weak spots of the interactions; or b) the decrease of the binding (negative mutations) conserving the weak spots, and mutating the hot spots of interactions.

## ACKNOWLEDGMENT

MDG was supported by a FIRC-AIRC fellowship for Italy (id. 22318). This work was supported by the Italian Ministry of Education, University and Research MIUR – SIR Programme no. RBSI149ZN9-BIOTAXI funded to MC.

## REFERENCES

[1] M. Calvaresi, F. Zerbetto, The devil and holy water: protein and carbon nanotube hybrids, Acc. Chem. Res. 46 (2013) 2454–2463.

[2] S. Marchesan, M. Prato, Under the lens: carbon nanotube and protein interaction at the nanoscale, Chem. Commun. 51 (2015) 4347–4359.

[3] F. De Leo, A. Magistrato, D. Bonifazi, Interfacing proteins with graphitic nanomaterials: from spontaneous attraction to tailored assemblies, Chem. Soc. Rev. 44 (2015) 6916–6953.

[4] D. Umadevi, S. Panigrahi, G.N. Sastry, Noncovalent interaction of carbon nanostructures, Acc. Chem. Res. 47 (2014) 2574–2581.

[5] S.F. Oliveira, G. Bisker, N.A. Bakh, S.L. Gibbs, M.P. Landry, M.S. Strano, Protein functionalized carbon nanomaterials for biomedical applications, Carbon. 95 (2015) 767–779.

[6] A. Antonucci, J. Kupis-Rozmysłowicz, A.A. Boghossian, Noncovalent protein and peptide functionalization of single-walled carbon nanotubes for biodelivery and optical sensing applications, ACS Appl. Mater. Interfaces. 9 (2017) 11321–11331.

[7] X. Cui, S. Xu, X. Wang, C. Chen, The nano-bio interaction and biomedical applications of carbon nanomaterials, Carbon 138 (2018) 436–450.

[8] K. Matsuura, T. Saito, T. Okazaki, S. Ohshima, M. Yumura, S. Iijima, Selectivity of water-soluble proteins in single-walled carbon nanotube dispersions, Chem. Phys. Lett. 429 (2006) 497–502.

[9] M. Calvaresi, S. Furini, C. Domene, A. Bottoni, F. Zerbetto, Blocking the Passage: $C_{60}$ Geometrically Clogs $K^+$ Channels, ACS Nano 9 (2015) 4827–4834.

[10] M. Calvaresi, A. Bottoni, F. Zerbetto, Thermodynamics of binding between proteins and carbon nanoparticles: the case of $C_{60}$@lysozyme, J. Phys. Chem. C. 119 (2015) 28077–28082.

[11] G. Grigoryan, Y.H. Kim, R. Acharya, K. Axelrod, R.M. Jain, L. Willis, M. Drndic, J.M. Kikkawa, W.F. DeGrado, Computational design of virus-like protein assemblies on carbon nanotube surfaces, Science 332 (2011) 1071–1076.

[12] K.-H. Kim, D.-K. Ko, Y.-T. Kim, N.H. Kim, J. Paul, S.-Q. Zhang, C.B. Murray, R. Acharya, W.F. DeGrado, Y.H. Kim, G. Grigoryan, Protein-directed self-assembly of a fullerene crystal, Nat. Commun. 7 (2016) 11429.

[13] S. Wang, E.S. Humphreys, S.-Y. Chung, D.F. Delduco, S.R. Lustig, H. Wang, K.N. Parker, N.W. Rizzo, S. Subramoney, Y.M. Chiang, A. Jagota, Peptides with selective affinity for carbon nanotubes, Nat. Mater. 2 (2003) 196.

[14] S. Brown, T.S. Jespersen, J. Nygard, A Genetic analysis of carbon-nanotube-binding proteins, Small 4 (2008) 416.

[15] M. Calvaresi, F. Zerbetto, Baiting proteins with $C_{60}$ ACS Nano 4 (2010) 2283–99.

[16] M. Calvaresi, F. Zerbetto, Fullerene sorting proteins, Nanoscale 3 (2011) 2873-2881.

[17] L. Ahmed, B. Rasulev, S. Kar, P. Krupa, M.A. Mozolewska, J. Leszczynski, Inhibitors or toxins? Large library target-specific screening of fullerene-based nanoparticles for drug design purpose., Nanoscale 9 (2017) 10263–10276.

[18] B.K. Shoichet, Virtual screening of chemical libraries, Nature. 432 (2004) 862–865.

[19] X. Xu, M. Huang, X. Zou, Docking-based inverse virtual screening: methods, applications, and challenges, Biophys. Reports. 4 (2018) 1–16.

[20] Y.Z. Chen, D.G. Zhi, Ligand-protein inverse docking and its potential use in the computer search of protein targets of a small molecule., Proteins. 43 (2001) 217–226.

[21] T.A. Ratnikova, P. Nedumpully Govindan, E. Salonen, P.C. Ke, In vitro polymerization of microtubules with a fullerene derivative, ACS Nano. 5 (2011) 6306–6314.

[22] L. Ahmed, B. Rasulev, M. Turabekova, D. Leszczynska, J. Leszczynski, Receptor- and ligand-based study of fullerene analogues: comprehensive computational approach including quantum-chemical, QSAR and molecular

docking simulations, Org. Biomol. Chem. 11 (2013) 5798–5808.

[23] P. Nedumpully Govindan, L. Monticelli, E. Salonen, Mechanism of *Taq* DNA polymerase inhibition by fullerene derivatives: insight from computer simulations, J. Phys. Chem. B. 116 (2012) 10676–10683.

[24] F. De Leo, J. Sgrignani, D. Bonifazi, A. Magistrato, Structural and dynamic properties of monoclonal antibodies immobilized on CNTs: a computational study, Chem. - A Eur. J. 19 (2013) 12281–12293.

[25] M. Calvaresi, S. Hoefinger, F. Zerbetto, Probing the structure of lysozyme-carbon-nanotube hybrids with molecular dynamics, Chem. - A Eur. J. 18 (2012) 4308–4313. doi:10.1002/chem.201102703.

[26] M. Turabekova, B. Rasulev, M. Theodore, J. Jackman, D. Leszczynska, J. Leszczynski, Immunotoxicity of nanoparticles: a computational study suggests that CNTs and $C_{60}$ fullerenes might be recognized as pathogens by Toll-like receptors, Nanoscale 6 (2014) 3488–3495.

[27] M. Calvaresi, F. Arnesano, S. Bonacchi, A. Bottoni, V. Calò, S. Conte, G. Falini, S. Fermani, M. Losacco, M. Montalti, G. Natile, L. Prodi, F. Sparla, F. Zerbetto, $C_{60}$@Lysozyme: direct observation by nuclear magnetic resonance of a 1:1 fullerene protein adduct., ACS Nano 8 (2014) 1871–1877.

[28] H. Yilmaz, L. Ahmed, B. Rasulev, J. Leszczynski, Application of ligand- and receptor-based approaches for prediction of the HIV-RT inhibitory activity of fullerene derivatives, J. Nanoparticle Res. 18 (2016) 123.

[29] X. Wu, S.-T. Yang, H. Wang, L. Wang, W. Hu, A. Cao, Y. Liu, Influences of the size and hydroxyl number of fullerenes/fullerenols on their interactions with proteins., J. Nanosci. Nanotechnol. 10 (2010) 6298–304.

[30] M. Chen, X. Qin, J. Li, G. Zeng, Probing molecular basis of single-walled

carbon nanotube degradation and nondegradation by enzymes based on manganese peroxidase and lignin peroxidase, RSC Adv. 6 (2016) 3592–3599.

[31] H. Shams, B.D. Holt, S.H. Mahboobi, Z. Jahed, M.F. Islam, K.N. Dahl, M.R.K. Mofrad, Actin reorganization through dynamic interactions with single-wall carbon nanotubes, ACS Nano. 8 (2014) 188–197.

[32] R. Marega, F. De Leo, F. Pineux, J. Sgrignani, A. Magistrato, A.D. Naik, Y. Garcia, L. Flamant, C. Michiels, D. Bonifazi, Functionalized Fe-filled multiwalled carbon nanotubes as multifunctional scaffolds for magnetization of cancer cells, Adv. Funct. Mater. 23 (2013) 3173–3184

[33] T. Mesarič, L. Baweja, B. Drašler, D. Drobne, D. Makovec, P. Dušak, A. Dhawan, K. Sepčić, Effects of surface curvature and surface characteristics of carbon-based nanomaterials on the adsorption and activity of acetylcholinesterase, Carbon 62 (2013) 222–232.

[34] L. Ren, D. Yan, W. Zhong, Enhanced enzyme activity through electron transfer between single-walled carbon nanotubes and horseradish peroxidase, Carbon 50 (2012) 1303–1310.

[35] Z. Zhu, Y. Wang, Y. Kang, H. Zhang, Z. Zhang, Z. Fei, J. Cao, Graphene oxide destabilizes myoglobin and alters its conformation, Carbon 114 (2017) 449–456.

[36] S. H. Friedman, P. S. Ganapathi, Y. Rubin, G. L. Kenyon, Optimizing the binding of fullerene inhibitors of the HIV-1 protease through predicted increases in hydrophobic desolvation, 41 (1998) 2424-2429.

[37] H. Benyamini, A. Shulman-Peleg, H.J. Wolfson, B. Belgorodsky, L. Fadeev, M. Gozin, Interaction of $C_{60}$-fullerene and carboxyfullerene with proteins: docking and binding site alignment, Bioconjugate Chem. 17 (2006) 378–386.

[38] B. Belgorodsky, L. Fadeev, J. Kolsenik, M. Gozin, Biodelivery of a fullerene derivative, Bioconjugate Chem. 18 (2007) 1095–1100.

[39] S.-T. Yang, H. Wang, L. Guo, Y. Gao, Y. Liu, A. Cao, Interaction of fullerenol with lysozyme investigated by experimental and computational approaches, Nanotechnology. 19 (2008) 395101.

[40] S. Durdagi, C.T. Supuran, T.A. Strom, N. Doostdar, M.K. Kumar, A.R. Barron, T. Mavromoustakos, M.G. Papadopoulos, *In silico* drug screening approach for the design of magic bullets: a successful example with anti-HIV fullerene Derivatized Amino Acids, J. Chem. Inf. Model. 49 (2009) 1139–1143.

[41] Z. Gao, H. Li, H. Zhang, X. Liu, L. Kang, X. Luo, W. Zhu, K. Chen, X. Wang, H. Jiang, PDTD: a web-accessible protein database for drug target identification, BMC Bioinformatics. 9 (2008) 104.

[42] S. Genheden, U. Ryde, The MM/PBSA and MM/GBSA methods to estimate ligand-binding affinities, Expert Opin. Drug Discov. 10 (2015) 449–461.

[43] C. Wang, D. Greene, L. Xiao, R. Qi, R. Luo, Recent Developments and Applications of the MMPBSA Method, Front. Mol. Biosci. 4 (2017) 87.

[44] D. Ma, X.Y. Meng, D.R. Bell, S. Liu, R. Zhou, Inhibition of CYP2C8 by metallofullerenol $Gd@C_{82}(OH)_{22}$ through blocking substrate channels and substrate recognition sites, Carbon 127 (2018) 667–675.

[45] F. Bologna, E.J. Mattioli, A. Bottoni, F. Zerbetto, M. Calvaresi, Interactions between endohedral metallofullerenes and proteins: the $Gd@C_{60}$ –lysozyme model, ACS Omega. 3 (2018) 13782–13789.

[46] D. Schneidman-Duhovny, Y. Inbar, V. Polak, M. Shatsky, I. Halperin, H. Benyamini, A. Barzilai, O. Dror, N. Haspel, R. Nussinov, H.J. Wolfson, Taking geometry to its edge: Fast unbound rigid (and hinge-bent) docking,

Proteins. 52 (2003) 107–112.

[47] C. Zhang, G. Vasmatzis, J.L. Cornette, C. DeLisi, Determination of atomic desolvation energies from the structures of crystallized proteins, J. Mol. Biol. 267 (1997) 707–726.

[48] N. Andrusier, R. Nussinov, H.J. Wolfson, FireDock: Fast interaction refinement in molecular docking, Proteins. 69 (2007) 139–159.

[49] C.L. Kingsford, B. Chazelle, M. Singh, Solving and analyzing side-chain positioning problems using linear and integer programming, Bioinformatics. 21 (2005) 1028–1039.

[50] S.S. Karajanagi, A. Vertegel, A. Ravi, S. Kane, J.S. Dordick, Structure and Function of Enzymes Adsorbed onto Single-Walled Carbon Nanotubes, Langmuir. 20 (2004) 11594–11599.

[51] D.A. Case, T.A. Darden, E.T. Cheatham, C.L. Simmerling, J. Wang, R.E. Duke, R. Luo, R.C. Walker, W. Zhang, K.M. Merz, B. Roberts, S. Hayik, A. Roitberg, G. Seabra, J. Swails, A.W. Götz, I. Kolossváry, K. F.Wong, F. Paesani, J. Vanicek, R. M.Wolf, J. Liu, X. Wu, S.R. Brozell, T. Steinbrecher, H. Gohlke, Q. Cai, X. Ye, J. Wang, M.-J. Hsieh, G. Cui, D.R. Roe, D.H. Mathews, M.G. Seetin, R. Salomon-Ferrer, V.B. C. Sagui, T. Luchko, S. Gusarov, A. Kovalenko, P.A. Kollman, AMBER 12, (2012).

[52] D. Bedrov, G.D. Smith, H. Davande, W. Li, Passive transport of C60 fullerenes through a lipid membrane: A molecular dynamics simulation study, J. Phys. Chem. B. 112 (2008) 2078–2084.

[53] L. Li, D. Bedrov, G.D. Smith, Water-induced interactions between carbon nanoparticles, J. Phys. Chem. B. 110 (2006) 10509–10513.

[54] M. Calvaresi, S. Hoefinger, F. Zerbetto, Probing the structure of lysozyme-

carbon-nanotube hybrids with molecular dynamics, Chem. - A Eur. J. 18 (2012) 4308-4313.

[55] M. Calvaresi, A. Bottoni, F. Zerbetto, Thermodynamics of binding between proteins and carbon nanoparticles: the case of $C_{60}$@lysozyme, J. Phys. Chem. C. 119 (2015) 28077-28082.

[56] S.M. Tomásio, T.R. Walsh, Modeling the binding affinity of peptides for graphitic surfaces. Influences of aromatic content and interfacial shape, J. Phys. Chem. C. 113 (2009) 8778–8785.

[57] V. Tsui, D.A. Case, Theory and applications of the generalized born solvation model in macromolecular simulations, Biopolymers. 56 (2000) 275–291.

[58] X. Zou, Y. Sun, I.D. Kuntz, Inclusion of solvation in ligand binding free energy calculations using the generalized-born model, J. Am. Chem. Soc. 121 (1999) 8033-8043.

[59] M. Nicoletti, C. Capodanno, C. Gambarotti, E. Fasoli, Proteomic investigation on bio-corona of functionalized multi-walled carbon nanotubes, Biochim. Biophys. Acta - Gen. Subj. 1862 (2018) 2293–2303.

[60] G. Candiano, V. Dimuccio, M. Bruschi, L. Santucci, R. Gusmano, E. Boschetti, P.G. Righetti, G.M. Ghiggeri, Combinatorial peptide ligand libraries for urine proteome analysis: Investigation of different elution systems, Electrophoresis. 30 (2009) 2405-2411.

[61] A. Shevchenko, M. Wilm, O. Vorm, M. Mann, Mass spectrometric sequencing of proteins from silver-stained polyacrylamide gels, Anal. Chem. 68 (1996) 850-858.

[62] K.H. Park, M. Chhowalla, Z. Iqbal, F. Sesti, Single-walled carbon nanotubes are a new class of ion channel blockers, J. Biol. Chem. 278 (2003) 50212–

50216.

[63] C. Ingrosso, G.V. Bianco, P. Lopalco, M. Tamborra, M.L. Curri, A. Corcelli, G. Bruno, A. Agostiano, P. Siciliano, M. Striccoli, Surface chemical functionalization of single walled carbon nanotubes with a bacteriorhodopsin mutant, Nanoscale. 4 (2012) 6434-6441.

[64] R. El-Sayed, K. Bhattacharya, Z. Gu, Z. Yang, J.K. Weber, H. Li, K. Leifer, Y. Zhao, M.S. Toprak, R. Zhou, B. Fadeel, Single-walled carbon nanotubes inhibit the cytochrome P450 enzyme, CYP3A4, Sci. Rep. 6 (2016) 21316.

[65] D. Tasis, N. Tagmatarchis, A. Bianco, M. Prato, Chemistry of carbon nanotubes, Chem. Rev. 106 (2006) 1105–1136.

[66] A. Hirsch, Functionalization of single-walled carbon nanotubes, Angew. Chemie Int. Ed. 41 (2002) 1853-1859.

[67] T. Premkumar, R. Mezzenga, K.E. Geckeler, Carbon nanotubes in the liquid phase: addressing the issue of dispersion, Small. 8 (2012) 1299–1313.

[68] M. Calvaresi, M. Dallavalle, F. Zerbetto, Wrapping nanotubles with micelles, hemimicelles, and cylindrical micelles, Small. 5 (2009) 2191–2198.

[69] D.M. Guldi, M. Holzinger, A. Hirsch, V. Georgakilas, M. Prato, First comparative emission assay of single-wall carbon nanotubes—solutions and dispersions, Chem. Commun. 3 (2003) 1130–1131.

[70] S.S. Karajanagi, H. Yang, P. Asuri, E. Sellitto, J.S. Dordick, R.S. Kane, Protein-assisted solubilization of single-walled carbon nanotubes, Langmuir. 22 (2006) 1392–1395.

[71] D. Nepal, K.E. Geckeler, pH-Sensitive dispersion and debundling of single-walled carbon nanotubes: lysozyme as a tool, Small. 2 (2006) 406–412.

[72] D. Nepal, K.E. Geckeler, Proteins and carbon nanotubes: close encounter in

water, Small. 3 (2007) 1259–1265.

[73] P. Goldberg-Oppenheimer, O. Regev, Exploring a nanotube dispersion mechanism with gold-labeled proteins via cryo-TEM imaging, Small. 3 (2007) 1894–1899.

[74] M. Saint-Cricq, J. Carrete, C. Gaboriaud, E. Gravel, E. Doris, N. Thielens, N. Mingo, W.L. Ling, Human immune protein C1q selectively disaggregates carbon nanotubes, Nano Lett. 17 (2017) 3409–3415.

[75] J. Zhong, L. Song, J. Meng, B. Gao, W. Chu, H. Xu, Y. Luo, J. Guo, A. Marcelli, S. Xie, Z. Wu, Bio-nano interaction of proteins adsorbed on single-walled carbon nanotubes, Carbon 47 (2009) 967–973.

[76] Z. Wang, Y. Wang, Y. Huang, S. Li, S. Feng, H. Xu, M. Qiao, Characterization and application of hydrophobin-dispersed multi-walled carbon nanotubes, Carbon 48 (2010) 2890–2898.

[77] N.E. Kallmyer, T. Huynh, J.C. Graves, J. Musielewicz, D. Tamiev, N.F. Reuel, Influence of sonication conditions and wrapping type on yield and fluorescent quality of noncovalently functionalized single-walled carbon nanotubes, Carbon 139 (2018) 609–613.

[78] E.M. Pérez, N. Martín, π–π interactions in carbon nanostructures, Chem. Soc. Rev. 44 (2015) 6425–6433.

[79] E.M. Pérez, N. Martín, Curves ahead: molecular receptors for fullerenes based on concave–convex complementarity, Chem. Soc. Rev. 37 (2008) 1512–1519.

[80] M.J. O'Connell, S.M. Bachilo, C.B. Huffman, V.C. Moore, M.S. Strano, E.H. Haroz, K.L. Rialon, P.J. Boul, W.H. Noon, C. Kittrell, J. Ma, R.H. Hauge, R.B. Weisman, R.E. Smalley, Band gap fluorescence from individual single-walled carbon nanotubes, Science,. 297 (2002) 593–596.

[81] Z. He, J. Zhou, Probing carbon nanotube-amino acid interactions in aqueous solution with molecular dynamics simulations, Carbon 78 (2014) 500–509.

[82] H. Nie, H. Wang, A. Cao, Z. Shi, S.-T. Yang, Y. Yuan, Y. Liu, Diameter-selective dispersion of double-walled carbon nanotubes by lysozyme, Nanoscale. 3 (2011) 970-973.

[83] F. Karchemsky, E. Drug, E. Mashiach-Farkash, L. Fadeev, H.J. Wolfson, M. Gozin, O. Regev, Diameter-selective dispersion of carbon nanotubes by β-lactoglobulin whey protein, Colloids Surfaces B Biointerfaces. 112 (2013) 16–22.

[84] P. Asuri, S.S. Karajanagi, H. Yang, T.J. Yim, R.S. Kane, J.S. Dordick, Increasing protein stability through control of the nanoscale environment, Langmuir. 22 (2006) 5833-5836.

[85] D.W. Horn, G. Ao, M. Maugey, C. Zakri, P. Poulin, V.A. Davis, Dispersion state and fiber toughness: antibacterial lysozyme-single walled carbon nanotubes, Adv. Funct. Mater. 23 (2013) 6082–6090.

[86] D.W. Horn, K. Tracy, C.J. Easley, V.A. Davis, Lysozyme dispersed single-walled carbon nanotubes: interaction and activity, J. Phys. Chem. C. 116 (2012) 10341–10348.

[87] M. Fioroni, T. Dworeck, F. Rodríguez-Ropero, ß-Barrel Channel Proteins as Tools in Nanotechnology: Biology, Basic Science and Advanced Applications. **2013**, *Springer Publishing Company.*

[88] D. Pantarotto, C.D. Partidos, J. Hoebeke, F. Brown, E. Kramer, J.P. Briand, S. Muller, M. Prato, A. Bianco, Immunization with peptide-functionalized carbon nanotubes enhances virus-specific neutralizing antibody responses, Chem. Biol. 10 (2003) 961.

[89] D.A. Scheinberg, M.R. McDevitt, T. Dao, J.J. Mulvey, E. Feinberg, S. Alidori, Carbon nanotubes as vaccine scaffolds, Adv. Drug Deliv. Rev. 65 (2013) 2016–2022.

[90] A. Battigelli, C. Ménard-Moyon, A. Bianco, Carbon nanomaterials as new tools for immunotherapeutic applications, J. Mater. Chem. B. 2 (2014) 6144–6156.

[91] T.R. Fadel, T.M. Fahmy, Immunotherapy applications of carbon nanotubes: From design to safe applications, Trends Biotechnol. 32 (2014) 198-209.

[92] N. Cai, C.C. Wong, Y.X. Gong, S.C.W. Tan, V. Chan, K. Liao, Modulating cell adhesion dynamics on carbon nanotube monolayer engineered with extracellular matrix proteins, ACS Appl. Mater. Interfaces. 2 (2010) 1038–1047.

[93] K. Tan, J.M. Casasnovas, J.H. Liu, M.J. Briskin, T.A. Springer, J.H. Wang, The structure of immunoglobulin superfamily domains 1 and 2 of MAdCAM-1 reveals novel features important for integrin recognition, Structure. 6 (1998) 793–801.

[94] K. Kostarelos, A. Bianco, M. Prato, Promises, facts and challenges for carbon nanotubes in imaging and therapeutics, Nat. Nanotechnol. 4 (2009) 627–633.

[95] A. Bianco, K. Kostarelos, M. Prato, Applications of carbon nanotubes in drug delivery, Curr. Opin. Chem. Biol. 9 (2005) 674–679.

[96] L. Lacerda, S. Raffa, M. Prato, A. Bianco, K. Kostarelos, Cell-penetrating CNTs for delivery of therapeutics, Nano Today. 2 (2007) 38–43.

[97] S.K. Vashist, D. Zheng, G. Pastorin, K. Al-Rubeaan, J.H.T. Luong, F.S. Sheu, Delivery of drugs and biomolecules using carbon nanotubes, Carbon 49 (2011) 4077–4097.

[98] T. Da Ros, A. Ostric, F. Andreola, M. Filocamo, M. Pietrogrande, F. Corsolini, M. Stroppiano, S. Bruni, A. Serafino, S. Fiorito, Carbon nanotubes as nanovectors for intracellular delivery of laronidase in Mucopolysaccharidosis type I, Nanoscale. 10 (2018) 657–665.

[99] C. Caoduro, R. Kacem, K. Boukari, F. Picaud, C.H. Brachais, D. Monchaud, C. Borg, H. Boulahdour, T. Gharbi, R. Delage-Mourroux, E. Hervouet, M. Pudlo, Carbon nanotube - protamine hybrid: evaluation of DNA cell penetration, Carbon 96 (2016) 742–752.

[100] P. Chakravarty, R. Marches, N.S. Zimmerman, A.D.-E. Swafford, P. Bajaj, I.H. Musselman, P. Pantano, R.K. Draper, L.S. Vitetta, Thermal ablation of tumor cells with antibody-functionalized single-walled carbon nanotubes, Proc. Natl. Acad. Sci. U.S.A. 105 (2008) 8697.

[101] C. Fabbro, H. Ali-Boucetta, T. Da Ros, K. Kostarelos, A. Bianco, M. Prato, Targeting carbon nanotubes against cancer, Chem. Commun. 48 (2012) 3911–3926.

[102] F. Pineux, R. Marega, A. Stopin, A. La Torre, Y. Garcia, E. Devlin, C. Michiels, A. N. Khlobystov, D. Bonifazi, Biotechnological promises of Fe-filled CNTs for cell shepherding and magnetic fluid hyperthermia applications, Nanoscale. 7 (2015) 20474-20488.

[103] S.Y. Kim, E.-S. Choi, H.-J. Lee, C. Moon, E. Kim, Transthyretin as a new transporter of nanoparticles for receptor-mediated transcytosis in rat brain microvessels, Colloids Surfaces B Biointerfaces. 136 (2015) 989–996.

[104] C. Ge, J. Du, L. Zhao, L. Wang, Y. Liu, D. Li, Y. Yang, R. Zhou, Y. Zhao, Z. Chai, C. Chen, Binding of blood proteins to carbon nanotubes reduces cytotoxicity., Proc. Natl. Acad. Sci. U. S. A. 108 (2011) 16968–16973.

[105] Y. Zhu, W. Li, Q. Li, Y. Li, Y. Li, X. Zhang, Q. Huang, Effects of serum proteins on intracellular uptake and cytotoxicity of carbon nanoparticles, Carbon 47 (2009) 1351–1358.

[106] Y. Cheng, D. Li, B. Ji, X. Shi, H. Gao, Structure-based design of carbon nanotubes as HIV-1 protease inhibitors: atomistic and coarse-grained simulations, J. Mol. Graph. Model. 29 (2010) 171–177.

[107] Z. Zhang, B. Wang, B. Wan, L. Yu, Q. Huang, Molecular dynamics study of carbon nanotube as a potential dual-functional inhibitor of HIV-1 integrase, Biochem. Biophys. Res. Commun. 436 (2013) 650–654.

[108] D. Iannazzo, A. Pistone, S. Galvagno, S. Ferro, L. De Luca, A.M. Monforte, T. Da Ros, C. Hadad, M. Prato, C. Pannecouque, Synthesis and anti-HIV activity of carboxylated and drug-conjugated multi-walled carbon nanotubes, Carbon 82 (2015) 548–561.

[109] C. Salvador-Morales, P. Townsend, E. Flahaut, C. Vénien-Bryan, A. Vlandas, M.L.H. Green, R.B. Sim, Binding of pulmonary surfactant proteins to carbon nanotubes; potential for damage to lung immune defense mechanisms, Carbon N. Y. 45 (2007) 607–617.

[110] S. Kraszewski, F. Picaud, I. Elhechmi, T. Gharbi, C. Ramseyer, How long a functionalized carbon nanotube can passively penetrate a lipid membrane, Carbon 50 (2012) 5301–5308.

[111] L. Lacerda, H. Ali-Boucetta, S. Kraszewski, M. Tarek, M. Prato, C. Ramseyer, K. Kostarelos, A. Bianco, How do functionalized carbon nanotubes land on, bind to and pierce through model and plasma membranes, Nanoscale. 5 (2013) 10242–10250.

[112] S. Höfinger, M. Melle-Franco, T. Gallo, A. Cantelli, M. Calvaresi, J.A.N.F.

Gomes, F. Zerbetto, A computational analysis of the insertion of carbon nanotubes into cellular membranes, Biomaterials. 32 (2011) 7079-7085.

[113] M. Pumera, The electrochemistry of carbon nanotubes: Fundamentals and applications, Chem. - A Eur. J. 15 (2009) 4970–4978.

[114] J. Wang, Carbon-nanotube based electrochemical biosensors: a review, Electroanalysis 17 (2005) 7–14.

[115] Y. Choi, I.S. Moody, P.C. Sims, S.R. Hunt, B.L. Corso, I. Perez, G.A. Weiss, P.G. Collins, Single-molecule lysozyme dynamics monitored by an electronic circuit, Science 335 (2012) 319-324.

[116] K. Bradley, M. Briman, A. Star, G. Gruner, Charge transfer from adsorbed proteins, Nano Lett. 4 (2004) 253-256.

[117] B.L. Allen, P.D. Kichambare, A. Star, Carbon nanotube field-effect-transistor-based biosensors, Adv. Mater. 19 (2007) 1439–1451.

[118] A. Star, J.-C.P. Gabriel, K. Bradley, G. Grüner, Electronic detection of specific protein binding using nanotube FET devices, Nano Lett. 3 (2003) 459-463.

[119] L. Dong, A. Subramanian, B.J. Nelson, Carbon nanotubes for nanorobotics, Nano Today. 2 (2007) 12–21.

[120] D. Pantarotto, W.R. Browne, B.L. Feringa, Autonomous propulsion of carbon nanotubes powered by a multienzyme ensemble, Chem. Commun. 0 (2008) 1533–1535.

[121] K.J. Wise, N.B. Gillespie, J.A. Stuart, M.P. Krebs, R.R. Birge, Optimization of bacteriorhodopsin for bioelectronic devices, Trends Biotechnol. 20 (2002) 387–394.

[122] C.J. Serpell, K. Kostarelos, B.G. Davis, Can carbon nanotubes deliver on their promise in biology? Harnessing unique properties for unparalleled applications,

ACS Cent. Sci. 2 (2016) 190–200.

[123] S. Marchesan, K. Kostarelos, A. Bianco, M. Prato, The winding road for carbon nanotubes in nanomedicine, Mater. Today. 18 (2015) 12–19.

[124] C. Ménard-Moyon, K. Kostarelos, M. Prato, A. Bianco, Functionalized Carbon Nanotubes for Probing and Modulating Molecular Functions, Chem. Biol. 17 (2010) 107–115.

[125] E. Heister, E.W. Brunner, G.R. Dieckmann, I. Jurewicz, A.B. Dalton, Are carbon nanotubes a natural solution? Applications in biology and medicine, ACS Appl. Mater. Interfaces. 5 (2013) 1870–1891.

[126] M. Prato, K. Kostarelos, A. Bianco, Functionalized carbon nanotubes in drug design and discovery, Acc. Chem. Res. 41 (2008) 60–68.

[127] F. Trozzi, T.D. Marforio, A. Bottoni, F. Zerbetto, M. Calvaresi, Engineering the fullerene-protein interface by computational design: the sum is more than its parts, Isr. J. Chem. 57 (2017) 547–552.